ISMEj manuscript No.
(will be inserted by the editor)

Sustainability of spatially distributed bacteria-phage systems

Rasmus Skytte Eriksen[1] · Namiko Mitarai[1] · Kim Sneppen[1,*]

Received: date / Accepted: date

The authors declare no conflict of interest.

R. Eriksen
University of Copenhagen, Niels Bohr Institute, Blegdamsvej 17, 2100 Copenhagen, Denmark
Tel.: +45-42394313
E-mail: rasmus.eriksen@nbi.ku.dk

N. Mitarai
University of Copenhagen, Niels Bohr Institute, Blegdamsvej 17, 2100 Copenhagen, Denmark
Tel.: +45-35325402
E-mail: mitarai@nbi.ku.dk

K. Sneppen
University of Copenhagen, Niels Bohr Institute, Blegdamsvej 17, 2100 Copenhagen, Denmark
Tel.: +45-35325352
E-mail: sneppen@nbi.ku.dk

Abstract Virulent phages can expose their bacterial hosts to devastating epidemics, in principle opening for a complete elimination of their hosts. Although experiments indeed confirm large reduction of susceptible bacteria, there is no reports of complete extinctions. We here address this phenomenon from the perspective of spatial organization of bacteria and how this can influence the final survival of them. By modeling the transient dynamics of bacteria and phages when they are introduced into an environment with finite resources, we quantify how the spatial separation of initial bacterial positions and the self-protection of bacteria growing in spherical colonies favor bacterial survival. This suggest that spatial structures on the millimeter scale plays an important role in maintaining microbial diversity.

Keywords Microbial ecology · Predator-prey · Spatial structure · Percolation · Microcolony

1 Introduction

Naturally occurring bacteria live in spatially structured habitats: in the soil [1, 2], in our guts [3, 4] and even the oceans are locally variegated [5]. The spatial heterogeneity is in part generated by the diversity of the microbial world[6], in part by clusters of food sources, and in part caused by the fact that bacterial division leaves the offspring close to their "mother" and thereby often form microcolonies [7, 8, 9]. The spatial heterogeneity may in turn amplify itself through propagation of host specific phages, if these percolate devastating infections through the parts of space with most homogeneous distribution of their hosts [10].

Traditionally, phage-bacteria ecosystems are modeled by generalized versions of the classical Lotka-Volterra equations [11, 12, 13, 14, 15, 16, 17, 18, 19]. In its simplest form, such mass-action equations predict sustained oscillations

which becomes damped when one takes into account resource limitations. In contrast to the oscillating lynx-hare systems from macroscopic ecology [20], the microbial ecology experiments appear much more damped. In fact, with realistic parameters for phage infections [21] the Lotka-Volterra type equations predict that an invading phage typically cause a collapse to less than one bacteria from whatever realistic bacterial population we start with. This is clearly not seen in microbial experiments. Rather, after an initial collapse to a measurable fraction of susceptible bacteria [14] they ultimately grow and settle to a density predicted by the steady state of the generalized Lotka-Volterra equations.

The mass-action kinetics obviously ignore the spatial constraints, where for example propagating phages systematically tend to deplete nearby hosts and thus may be unable to reach more distant hosts before the phages decay. The presence of boundaries of bacterial colonies further add to these structured environments [22]. In this paper, we explore these constrained bacteria systematically as function of the initial distribution of bacterial hosts and their phages.

One useful model system for spatial systems of microbes is found in the human gut. For example, during faecal microbiota transplantation, new bacteria and phages are introduced to the patients gut in an attempt to restore diversity to the microbiome. The subsequent fate of a phage epidemic is played out in the spatially constrained environment consisting of bacteria that divide in relatively fixed positions, while potentially depleting the local nutrient as the population grows to the carrying capacity of the niche. The success of the treatment is reliant on the outcome of the phage epidemic, as their ability to control bacterial biomass can alter the composition of the transplanted matter[23]. The study of how phage and bacteria interact in spatially structured

environments is therefore part of designing effective phage-based or bacteria-based treatments.

2 Model and methods

Starting with an initial concentration of nutrient $n(t = 0\ h) = B_{max}$ that is measured in terms of the total density of bacteria it can be converted to, the mass-action equations between bacterial density, B, and phage density, P, reads [13, 14]:

$$\begin{aligned} \frac{dn}{dt} &= -\lambda B \frac{n}{n+K} \\ \frac{dB}{dt} &= \lambda B \frac{n}{n+K} - \eta BP \\ \frac{dP}{dt} &= (\beta - 1)\eta BP - \delta P \end{aligned} \tag{1}$$

where λ is the maximal bacterial growth rate, η is the adsorption rate for phages, β is the phage burst size, δ is the phage decay rate [21, 24]. K is the Monod constant [25] which determines at which concentration of nutrients the growth rate is halved.

These equations are modified from standard Lotka-Volterra equations by the depletion of food, and the associated parameterization of growth by the Monod equation. The above equations are the simplest way to model the development of bacteria-phage system in a fixed batch culture (eg. as used for temperate phage dynamics in [26]). Noticeably the model ignores the latency time between phage infection and cell lysis. This is easy to include, either through a time delay equation, or by introducing some intermediate infected states, I_k, between infection and lysis.

Including the latency of cell lysis, and the fact that bacteria grow in spatially separated colonies a more appropriate set of equations are:

$$
\begin{aligned}
\frac{dn}{dt} &= -\lambda B \frac{n}{n+K} + D_n \nabla^2 n \\
\frac{dB}{dt} &= \lambda B \frac{n}{n+K} - S(B, I, n_c, \zeta) \left[\eta \left(\frac{B+I}{n_c} \right)^{1/3} n_c P + \alpha\beta \frac{10}{\tau} I_{10} \frac{n}{n+K} \right] \\
\frac{dI_1}{dt} &= S(B, I, n_c, \zeta) \left[\eta \left(\frac{B+I}{n_c} \right)^{1/3} n_c P + \alpha\beta \frac{10}{\tau} I_{10} \frac{n}{n+K} \right] - \frac{10}{\tau} I_1 \frac{n}{n+K} \\
\frac{dI_i}{dt} &= \frac{10}{\tau} \frac{n}{n+K} \left(I_{i-1} - I_i \right) \quad i = 2, 3, ..., 10 \\
\frac{dP}{dt} &= (1-\alpha)\beta \frac{10}{\tau} I_{10} \frac{n}{n+K} - \delta P - \eta \left(\frac{B+I}{n_c} \right)^{1/3} n_c P + D_p \nabla^2 P
\end{aligned} \tag{2}
$$

where D_n and D_p are the diffusion constants for the nutrient and phages respectively. Here $D_n \sim 10^6 \mu m^2/h$ is much larger than $D_p \sim 10^4 \mu m^2/h$. The bacteria are constrained in space, and each initial bacteria grow to a colony of size $(B+I)/n_c$, where $n_c = B(t=0)$ is the density of the initial bacteria. When a phage is adsorbed to a colony, it does so with a rate that is proportional to the colony radius (hence the 1/3 exponent). However, when some bacteria in the colony are already infected, then only a fraction S of the infections leads to new infected states, since the accumulated infected cells exists on the surface of the colony and partially shields the uninfected cell from the phage attack [9]. This protection is defined by the shielding function S. In the Appendix, we investigated various shielding functions, and found that a shielding function on the form:

$$
\tilde{S}(B, I, n_c, \zeta) = \exp\left(-\tfrac{1}{\zeta} \left(\left(\tfrac{B+I}{n_c} \right)^{\frac{1}{3}} - \left(\tfrac{B}{n_c} \right)^{\frac{1}{3}} \right) \right),
$$

is a reasonable approximation. This shielding functions gives the probability that a diffusing phage passes through the absorbing surface of thickness

$\left(\frac{3V_0}{4\pi}\right)^{\frac{1}{3}}\left(\left(\frac{B+I}{n_c}\right)^{\frac{1}{3}}-\left(\frac{B}{n_c}\right)^{\frac{1}{3}}\right)$, where V_0 is the volume of a single bacterium. The parameter ζ is the typical distance the phage can penetrate before being adsorbed (in units of $\left(\frac{3V_0}{4\pi}\right)^{\frac{1}{3}}$). In the Appendix, we estimate ζ as a function of the phage adsorption coefficient via detailed simulations of colonies consisting of spherical bacteria, and find that for the diffusion limited case ζ is roughly 1.

Note that to match in the shielding in the small colony limit where $S(B, I, n_c, \zeta) = \frac{B}{B+I}$, we must force an upper limit on the shielding:

$$S(B, I, n_c, \zeta) = \min\left[\frac{B}{B+I},\ \ \tilde{S}(B, I, n_c, \zeta)\right]$$

The model in Eq. (2) also includes the latency time, of the infection cycle, which is obtained with the use of 10 intermediate infected states $I = \sum_{k=1}^{10} I_k$ between infection and final release of phages[27]. This correspond to an average latency time τ that varies $1/\sqrt{10} \sim 30\%$ between separate lysis events. When lysis occurs, the released phage has a high probability of reinfecting the colony, which is represented by the parameter α. A fraction $(1-\alpha)$ of the phage progeny escape from the colony and becomes free phages P, while a fraction α readsorbs to the colony by adsorbing to its bacteria.

We include space by simulating the equations in a 3-dimensional system of one cubic centimeter with grid size $\ell = 0.2\ mm$. This approach allows for different numbers of bacteria and phages in each of the $1.25 \cdot 10^5$ boxes in the lattice. In order to represent the behaviour of a larger system we use periodic boundary conditions.

The simulation starts by partitioning the initial bacteria into all the boxes randomly, thereby giving an initial bacteria number that varies between the boxes.

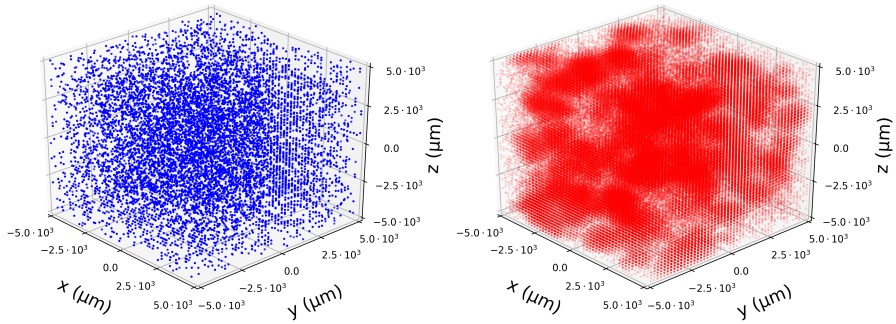

Fig. 1 Snapshot of simulation. The spatial distribution of bacteria (blue) and phages (red) at time $T = 7\ h$ starting from an initial $B = 10^4$ bacteria per ml and $P = 10^5$ phages per ml. The opacity of each point is proportional to $\log 10$ of the population in that point.

Every box is considered to be well-mixed, and therefore when a bacterium lyses, the fraction $(1-\alpha)$ of released phages are assumed to be distributed homogeneously in the local box of size ℓ. Phages can thus freely infect any colony in each box equally as given by the diffusion controlled reaction equation.

We solve the equations stochastically by treating each term in Eq. (2) as rates corresponding to events. At each time step, we compute the probability for every particle to undergo each event, and draw the number of occurrences from a Poisson distribution (see Appendix for details). Every box is solved independently, modulated by diffusion of food and phages between the boxes. The diffusion of phages is done by random walk of appropriate fractions of the phage population to neighboring lattice boxes. Nutrient diffusion is solved by using a discrete laplace operator (using the "forward time central space" scheme).

The problem contains two different timescales, that of bacteria and phages versus that of nutrient diffusion. In order to solve nutrient diffusion accurately we require that $D_n \frac{\Delta T}{\ell^2} \leq \frac{1}{6}$, which we obtain for time steps of size $\Delta T = 2 \cdot 10^{-3}\ h \sim 7\ s$.

An example of a simulation can be seen in Fig. 1.

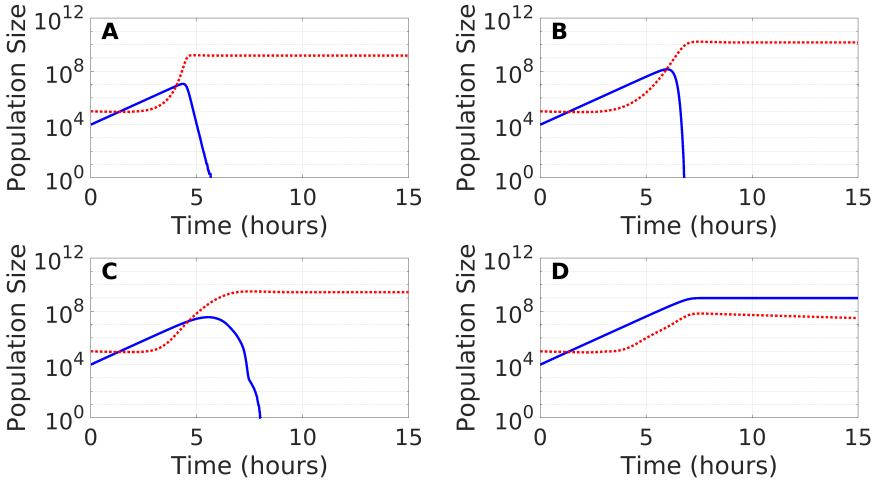

Fig. 2 Dynamics of bacteria and phages. The solid blue lines indicate the bacterial population, while the dotted red lines indicate the phage population. (A) Simple Lotka-Volterra. (B) Lotka-Volterra with a time-delay. (C) Lotka-Volterra model with time-delay and space. (D) Lotka-Volterra model with time-delay, space, and colony level protection. In all cases we start with the initial condition $B = 10^4$ bacteria per ml and $P = 10^5$ phages per ml, and assume a max production of $n(t = 0) = 10^9$ bacteria per ml.

3 Results

The model is simulated with four different levels of spatial detail. Each level shows the effects of the changes from the initial mass-action equations we presented in Eq. (1), to the full spatiotemporal model that also include protection due to colony formation.

Examples of simulations are illustrated in Fig. 2, where one can follow the trajectory of the system as described by the different levels of details: In (A) we solve Eq. (1), and observe how the phage quickly overwhelms the bacteria leading to the extinction of the bacteria. In (B) we solve Eq. (2) without the addition of space (one box with $\ell = 1\ cm$), and we also remove the effect of colony level protection by setting $n_c = B + I$, $S(B, I, n_c, \zeta) = \frac{B}{B+I}$, and $\alpha = 0$. This leaves us with a mass-action model like Eq. (1) but which includes the latency between phage infection and cell lysis. The latency of the lysis cycle delays the growth of phages, thereby leaving more time for bacteria to

grow. As a result, the bacteria reach a higher density and subsequently is exposed to a more dramatic collapse when phage population catches up. Thus the inclusion of the appropriate time delays predicts more unstable behavior, and is accordingly less in agreement with typical experiments than the simpler equation used in panel (A).

Panel (C) and (D) explores the two levels of spatial detail, both with the appropriate time delay due to latency. Panel (C) only introduce spatial variation and keep the restraints $n_c = B + I$, $S(B, I, n_c, \zeta) = \frac{B}{B+I}$, and $\alpha = 0$. The added heterogeneity of space further delays the extinction of the bacteria as different regions of space experience different phage densities. Panel (D) use the full model that includes colony level protection. One sees dramatic improvement in stability, with bacteria surviving to reach a steady state where normal phages cannot propagate. Notice that we do not model large plaque former like phages T7 here, as we assume that phage latency diverge with same Monod factor as the bacterial generation time (Eq. (2)). In fact, when including protection due to colony formation, the bacteria can only be eliminated when the initial phage load is high enough to eliminate bacteria before they form sufficiently large colonies.

Fig. 3 explores bacterial survival as function of initial density of phages and bacteria in the four levels of modeling detail. In each case, the simulation is initiated with bacterial and phage populations between 1 and 10^9 per ml. The spatial simulation consider 1 cm^3 coarse grained into boxes of dimension 0.2 mm, and a bacterial population of 10^5 per ml accordingly correspond to an average population of one bacteria per box. In each panel one can see a dark blue region that represents conditions where bacterial populations are entirely eliminated. For each model variant this “dead” region expands as simulation time is increased (going from left to right shows to the bacterial population at 5h, 10h and finally 15h). After 15h the nutrient is depleted in most cases.

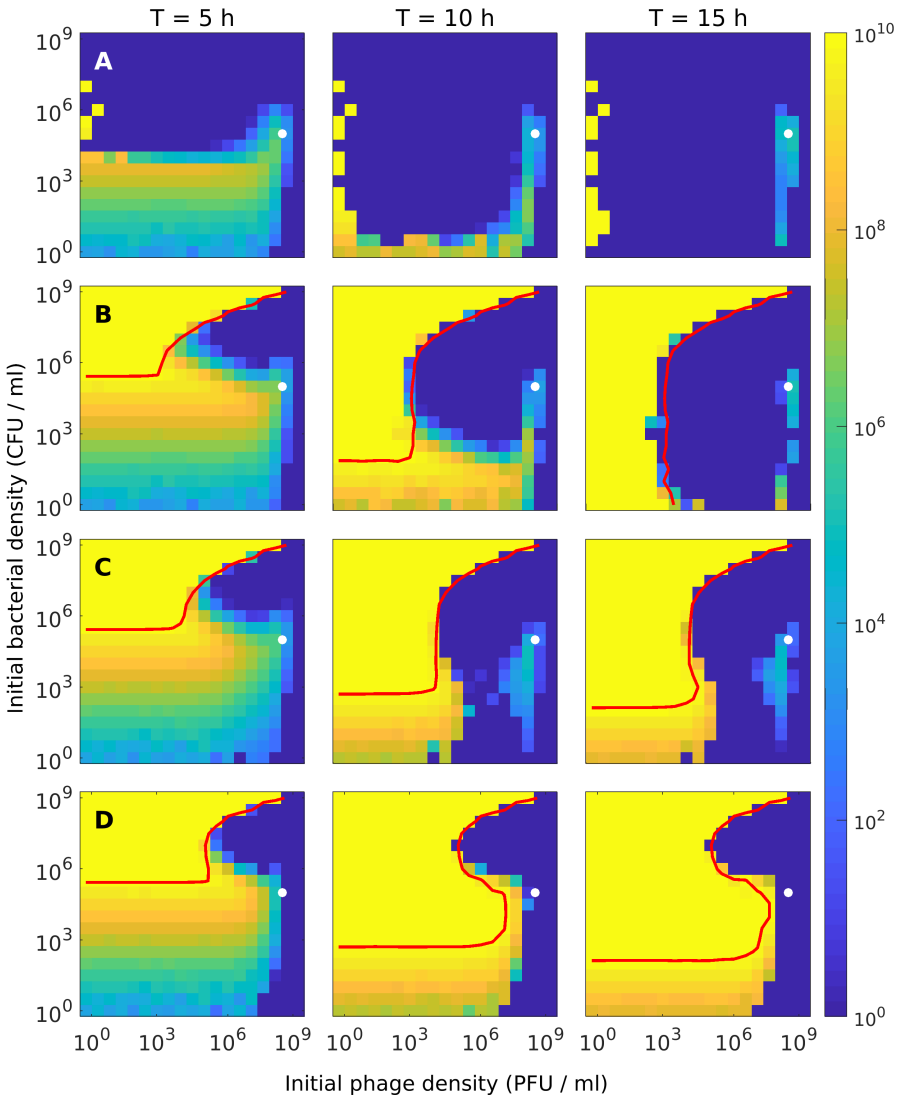

Fig. 3 Phase space plots of the surviving bacteria. The color shows the total bacterial population at the given time as a function of initial phage density and initial bacterial density. The red line indicate the nutrient contour $n = K$, where the growth rate is halved. The white dots indicate where $P = 2 \cdot 10^8$ / ml and $B = 10^5$ / ml. Each column show the dynamics at $T = 5$ h, $T = 10$ h, and $T = 15$ h respectively, while the rows indicate different models: A) Simple Lotka-Volterra. B) Lotka-Volterra with a time-delay. C) Lotka-Volterra model with time-delay and space. D) Lotka-Volterra model with time-delay, space, and colony level protection.

This is highlighted by the red line, marking conditions where $n = K$. Above this red line the accumulated number of bacterial divisions approaches the carrying capacity, and the system remains largely unchanging.

Fig. 3 (A) show that the fate of the bacterial populations is similar across a range of initial conditions where the phage eradicate the bacteria. In some cases we observe transient survival where bacterial growth balances death due to phages. In quantitative terms, the bacteria population is marginally sustained when the rate of phage adsorbing to bacteria is approximately equal to the rate of bacteria division, $\lambda B \sim \eta BP \Rightarrow P \approx \lambda/\eta = 2 \cdot 10^8 \ / \ ml$. Further, the phage population cannot increase when the rate of phage produced by lysis is less than the decay rate of the phage.

At the point where phage adsorption is balanced by the bacterial growth rate ($P \approx 2 \cdot 10^8 \ / \ ml$), the population of infected bacteria is approximately $I \approx \lambda B \tau$, which means that the phage production rate is approximately $\dot{P} \approx \beta\lambda B - \lambda B - \delta P$. For our parameter values, this is zero when $B \approx 10^5 \ / \ ml$. When initial B is larger than $10^5 \ / \ ml$, the phage population can grow from the beginning, whereas lower bacterial density means that phages cannot grow before bacterial population has increased. Around these critical densities, the phage does not grow sufficiently fast to repress the bacterial population within 15 h.

Fig. 3 (A) Shows that the initial Lotka-Volterra dynamics only predict long term survival, when the phage density is extremely low. Here the bacteria can reach carrying capacity and thus survive indefinitely, due to the phages decaying before adsorbing to the bacteria.

Fig. 3 (B) demonstrate that the latency time of phage infection enables the bacterial population to survive in a much larger region of initial conditions, compared to panel (A). This survival arises because the latency allow the bacterial population to deplete the nutrient before the phage population grows

large enough to exterminate the bacteria. This observation gives an addendum to our observation based on Fig. 2 (B): while latency leads to larger crashes of the bacterial population in some cases, it leads to long term survival in other cases.

Fig. 3 panels (C) and (D) demonstrate the moderating effects of space, where the initial conditions for long term survival for bacteria is greatly extended. The combination of sub-critical percolation at moderate levels of initial bacterial density (C), and the build up of sizable colonies (D) tend to provide for robust bacterial survival also in the region around $10^4 - 10^8$ initial phage per ml.

To test the model, we modify the setup to mimic the conditions used in the experiment performed in ref. [9]. There a number of *Escherichia coli* was suspended in a soft agar and plated onto petri dishes. After a time where each bacterial had grown to some small colony, the plates were sprayed with the virulent phage $P1_{vir}$, and the number of visible bacterial colonies were counted 16 hours later. In the experiment the formed bacterial colonies was about 1 cm apart, embedded in a soft agar of height $\approx 400\ \mu m$. These conditions is replicated by simulating a single bacterium inside a box of dimensions $10^4\ \mu m \times 10^4\ \mu m \times 400\ \mu m$. The phages are spawned in the XY plane at $Z = 400\ \mu m$, and we change the boundary condition in the Z axis from periodic to reflective. In addition, we increased the spatial resolution by setting $\ell = 0.1\ mm$ in order to better resolve the Z axis. The increased resolution requires the nutrient to be solved on a time scale of $\Delta T = 5 \cdot 10^{-4}\ h$. The shorter time scale means that computation time increases significantly. To remedy this situation, we exploit the fact that phages move on average $\sim \sqrt{2 \cdot D_P \cdot 16\ h} \approx 300\ \mu m$ during the experiment. We therefore only solve the phages in an area of $10^3\ \mu m \times 10^3\ \mu m \times 400\ \mu m$ centered on the colony. A visualization of the scenario is shown in Fig. 4 (A-B).

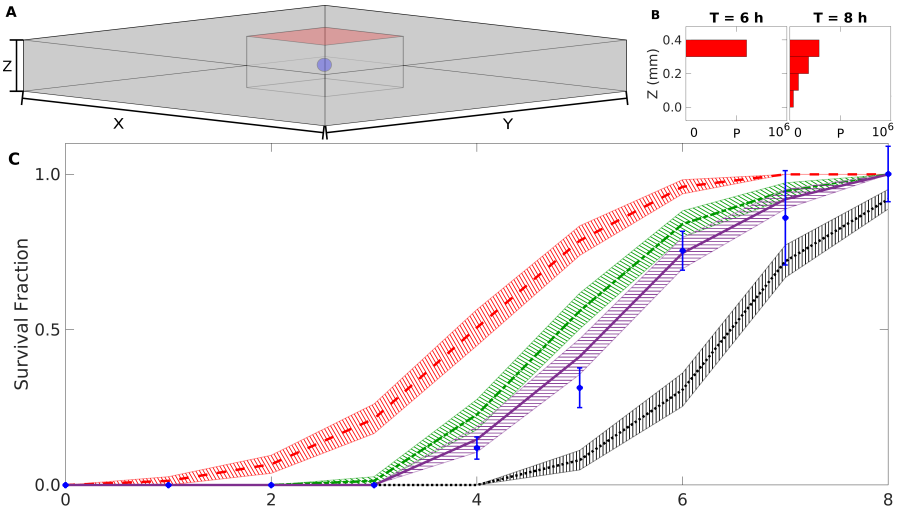

Fig. 4 Reproducing experiment. (A) Illustration of a simulation. The spatial distribution of phages (red) at time $T = 6.0\ h$ starting from a single bacterium and with $P = 6 \cdot 10^5$ phages being distributed at $Z = 400\ \mu m$ at time $T = 6.0\ h$. The location of the bacterial colony is shown by the blue dot. (B) The vertical distribution of phages at time $T = 6.0\ h$ and $T = 8\ h$. (C) The fraction of colonies which grows to visible size in experiments 16 hours after phage exposure (blue error-bars) [9] and the fraction of simulated colonies ($n = 75$) which produce more than $5{\cdot}10^5$ cells after 16 hours for $\zeta = 2.5$ (red dashed line), $\zeta = 5$ (green dash-dotted line), and $\zeta = 10$ (purple line). As a control, we include the prediction when the colony level protections are disabled (black dotted line). The hatched area around each line indicate the standard error. The simulation here uses P1 parameters[21, 9]: $\beta = 400$, $\delta = 0.1\ h^{-1}$, $\eta = 1.32 \cdot 10^4\ \mu m^3/h$, $\tau = 1\ h$, and parameters to match the experimental conditions[9]: Simulation volume of $400\ \mu m \times 10^4\ \mu m \times 10^4\ \mu m$, $D_P = 3000\ \mu m^2/h$ ($\sim$1/10 of phage-λ value) and $\lambda = 60/31\ h^{-1}$.

For each time, T_i, of phage spawning, we simulate 75 stochastic developments of a single bacterial colony and compute the fraction that have grown to visible size at $T_i + 16$ hours. A colony is defined as visible, if the number of produced cells is above $5{\cdot}10^5$, corresponding to a colony of radius $\approx 50\ \mu m$. Notice that we count cells produced and not the final alive cells, because dead cells also contribute to making the colony visible. Operationally the number of dead cells is counted by measuring consumed nutrient, $n(t = 0h) - n(t = 16h + T_i)$, which has been converted to biomass.

Fig. 4 (C) compare model prediction against the experimental observations [9]. When comparing the fraction of visible colonies in Fig. 4 (C), the simulation with $\zeta = 10$ reproduce the experimental result reasonably well, meaning

that phages typically penetrate through 5-10 layers of bacteria before final adsorption.

Since *Escherichia coli* has a volume of $V_0 \sim 1\ \mu m^3$, the parameter ζ gives the typical penetration depth: $\left(\frac{3V_0}{4\pi}\right)^{\frac{1}{3}} \zeta$.

Ref. [9] also derives a model of the critical radius, R_c, for a bacterial colony above which it can survive a phage attack. The model assumes the colony is spherical and that the phages can penetrate a fixed distance ΔR into the colony. The critical radius is predicted to be: $R_c = 3[1+(g\tau)^{-1}]\Delta R$. From their measurement of $R_c \approx 25\ \mu m$, we can estimate ΔR. Since the colony is small when survival is determined, we assume the nutrient depletion is negligible and set the effective bacterial growth rate $g = \lambda \frac{n_0}{n_0+K} = \frac{60}{31}\frac{5}{6}\ h^{-1} = 1.61\ h^{-1}$. Rearranging their prediction yields the following expression:

$$\Delta R = \frac{R_c}{3(1+(g\tau)^{-1})} \approx 5\ \mu m \tag{3}$$

This penetration depth corresponds to a value of $\zeta = 8.3$.

The fraction of surviving colonies is dependent on the value of the phage diffusion constant D_P. As we do not have an exact estimate of this parameter, we investigate how the survival fraction is affected by different diffusion constants. This is done in the Appendix, where we find that if the diffusion constant is large, the fraction of surviving colonies only match the experimental results when the shielding is strong (i.e. ζ small), but as the diffusion constant decreases, larger and larger values of ζ can reproduce the experiment.

4 Discussion

The main prediction of this paper is that space provides greatly increased robustness of phage-bacteria systems against dramatic collapses. This is in conceptual agreement with the constructed spatially study of [28] and further

suggest that even the supposedly well mixed environments of for example ref. [14] may be structured on microscopic scale.

Our study was simplified in multiple ways. In particular, we considered the survival of one bacterial strain exposed to one phage strain. This implicitly ignore nutrient depletion due to competing bacteria, a situation which typically will favour the long term survival of any particular strain of bacteria. Our model also ignored the fraction of bacteria that are resistant against a given phage [29]. If there is a fraction of about 10^{-5} to 10^{-6} bacterial mutants that lack the surface receptor used by the phage, a bacterial collapse will of course not be complete. Instead it will cause a large enough depletion to disturb of the bacterial composition, and would lead to dominance of strains that typically are growing substantially slower than the original strain (cost of resistance [30, 31]).

We have found no published experiments on phage-bacteria interactions that reported cases where the susceptible bacteria are completely eliminated. In this perspective the presented modeling is a step towards a better explanation, although it still predicts conditions where bacteria should be completely eliminated. Thus further modifications to our modeling could be needed, for example by allowing the phage infections to vary hugely between the different bacteria. Perhaps the widely acclaimed variability in bacterial gene expression is a desired trait, that allow some bacteria to be immune to phages for several generations [32, 33, 34].

Our equations (Eq. (2)) are an approximated treatment of a system which can have quite variable strain specific properties. For example, our diverging latency time with nutrient depletion means that phage do not prey on stationary state bacteria, an assumption that is mostly correct but would fail for example for phage T7 preying on *Escherichia coli*[35]. Note that spatial structure is still relevant in such a case, as shown in protection by biofilm that

hinder physical contact of phages to bacteria [36, 37]. Also the equations does not consider temperate phages, which would only induce a collapse of order 0.1 to 0.01 (typical recorded lysogeny frequencies [27]). The equations also does not consider delayed lysis, where for example the simultaneous infections by several T4 phages causes longer latency times[38]. Finally the treatment of bacterial colonies is simplified, as we have not yet obtained a complete understanding of their protective nature [9]. In terms of our model, perhaps the assumption of well mixed phages within each box of size 0.2 mm is doubtful, and the part of the model in Eq. (2) which describes readsorption of phage to the bacterial colony might well be improved.

A major factor in the strength of the protection mechanism is the parameter ζ which is a measure of the typical penetration depth of the phages. The ability of phages to penetrate bacterial colonies is likely to be dependent on several factors such as the geometry of the cells, the densities of the colonies, and whether or not the cells produce biofilm. Thereby this part of the phage protection should depend on the ability of the bacterial species to quorum sense and to collectively modify its own local environment.

The model highlight the importance of colony formation, and their ability to provide safe shelters. In fact, given that increasing colony sizes provide both local protection, and make phage percolation between colonies less likely, one should consider colony formation as a strategic option for both bacteria in the wild, our use of bacteria in industry or in human gut re-implantation, and in situations where one want to eliminate pathogenic bacteria by phage therapy.

Acknowledgements This work was supported by the European Research Council under the European Union's Seventh Framework Programme (FP/2007 2013)/ERC Grant Agreement n. 740704 and the Danish National Research Foundation (BASP: DNRF120).

Competing Interests

The authors declare no conflict of interest.

References

[1] Vigdis Torsvik, Jostein Goksøyr, and Frida Lise Daae. "High diversity in DNA of soil bacteria." In: *Applied and environmental microbiology* 56.3 (1990), pp. 782–787.

[2] Lionel Ranjard and Agnès Richaume. "Quantitative and qualitative microscale distribution of bacteria in soil". In: *Research in microbiology* 152.8 (2001), pp. 707–716.

[3] Manimozhiyan Arumugam, Jeroen Raes, Eric Pelletier, Denis Le Paslier, Takuji Yamada, Daniel R Mende, et al. "Enterotypes of the human gut microbiome". In: *nature* 473.7346 (2011), p. 174.

[4] Vanni Bucci and Joao B Xavier. "Towards predictive models of the human gut microbiome". In: *Journal of molecular biology* 426.23 (2014), pp. 3907–3916.

[5] Farooq Azam and Francesca Malfatti. "Microbial structuring of marine ecosystems". In: *Nat. Rev. Microbiol.* 5.10 (2007), pp. 782–791.

[6] Curtis A. Suttle. "Marine viruses - Major players in the global ecosystem". In: *Nature Reviews Microbiology* 5.10 (2007), pp. 801–812. DOI: 10.1038/nrmicro1750.

[7] W R Young, A J Roberts, and G Stuhne. "Reproductive pair correlations, Brownian bugs and plankton patches". In: *Nature* 412 (2001), p. 328.

[8] Xinxian Shao, Andrew Mugler, Justin Kim, Ha Jun Jeong, Bruce R Levin, and Ilya Nemenman. "Growth of bacteria in 3-d colonies". In: *PLOS Comput. Biol.* 13.7 (2017), e1005679.

[9] Rasmus Skytte Eriksen, Sine L Svenningsen, Kim Sneppen, and Namiko Mitarai. "A growing microcolony can survive and support persistent propagation of virulent phages". In: *Proceedings of the National Academy of Sciences* (2017), p. 201708954.

[10] Bradford P Taylor, Catherine J Penington, and Joshua S Weitz. "Emergence of increased frequency and severity of multiple infections by viruses due to spatial clustering of hosts". In: *Phys. Biol.* 13.6 (2017), p. 066014.

[11] Alfred J Lotka. "The frequency distribution of scientific productivity". In: *Journal of the Washington academy of sciences* 16.12 (1926), pp. 317–323.

[12] Vito Volterra. "Variations and fluctuations of the number of individuals in animal species living together". In: *ICES Journal of Marine Science* 3.1 (1928), pp. 3–51.

[13] Allan Campbell. "Conditions for the existence of bacteriophage". In: *Evolution* (1961), pp. 153–165.

[14] Bruce R Levin, Frank M Stewart, and Lin Chao. "Resource-limited growth, competition, and predation: a model and experimental studies with bacteria and bacteriophage". In: *Am. Nat.* 111.977 (1977), pp. 3–24.

[15] T Frede Thingstad. "Elements of a theory for the mechanisms controlling abundance, diversity, and biogeochemical role of lytic bacterial viruses in aquatic systems". In: *Limnol. Oceanogr.* 45.6 (2000), pp. 1320–1328.

[16] Joshua S Weitz, Hyman Hartman, and Simon A Levin. "Coevolutionary arms races between bacteria and bacteriophage". In: *Proceedings of the National Academy of Sciences of the United States of America* 102.27 (2005), pp. 9535–9540.

[17] Joshua S. Weitz and Jonathan Dushoff. "Alternative stable states in host - Phage dynamics". In: *Theoretical Ecology* 1.1 (2008), pp. 13–19. DOI: 10.1007/s12080-007-0001-1.

[18] Zhenyu Wang and Nigel Goldenfeld. "Fixed points and limit cycles in the population dynamics of lysogenic viruses and their hosts". In: *Physical Review E - Statistical, Nonlinear, and Soft Matter Physics* 82.1 (2010), pp. 1–18. DOI: 10.1103/PhysRevE.82.011918.

[19] Jan O Haerter, Namiko Mitarai, and Kim Sneppen. "Phage and bacteria support mutual diversity in a narrowing staircase of coexistence". In: *ISME J.* 8.11 (2014), pp. 2317–2326.

[20] Charles J Krebs, Rudy Boonstra, Stan Boutin, and Anthony RE Sinclair. "What Drives the 10-year Cycle of Snowshoe Hares? The ten-year cycle of snowshoe haresone of the most striking features of the boreal forestis a product of the interaction between predation and food supplies, as large-scale experiments in the yukon have demonstrated". In: *AIBS Bulletin* 51.1 (2001), pp. 25–35.

[21] Marianne De Paepe and François Taddei. "Viruses' life history: towards a mechanistic basis of a trade-off between survival and reproduction among phages". In: *PLoS Biol.* 4.7 (2006), e193.

[22] Silja Heilmann, Kim Sneppen, and Sandeep Krishna. "Coexistence of phage and bacteria on the boundary of self-organized refuges". In: *Proc. Natl. Acad. Sci. USA* 109.31 (2012), pp. 12828–12833.

[23] Tao Zuo, Sunny H Wong, Kelvin Lam, Rashid Lui, Kitty Cheung, Whitney Tang, et al. "Bacteriophage transfer during faecal microbiota transplantation in Clostridium difficile infection is associated with treatment outcome". In: *Gut* (2017), gutjnl–2017–313952. DOI: 10.1136/gutjnl-2017-313952.

[24] R T Noble and JA Fuhrman. "Virus decay and its causes in coastal waters." In: *Applied and Environmental Microbiology* 63.1 (1997), pp. 77–83.

[25] Jacques Monod. "The growth of bacterial cultures". In: *Annual Reviews in Microbiology* 3.1 (1949), pp. 371–394.

[26] Nathaniel D Maynard, Elsa W Birch, Jayodita C Sanghvi, Lu Chen, Miriam V Gutschow, and Markus W Covert. "A forward-genetic screen and dynamic analysis of lambda phage host-dependencies reveals an extensive interaction network and a new anti-viral strategy". In: *PLoS genetics* 6.7 (2010), e1001017.

[27] Namiko Mitarai, Stanley Brown, and Kim Sneppen. "Population dynamics of phage and bacteria in spatially structured habitats using Phage λ and Escherichia coli". In: *J. Bacteriol.* 198.12 (2016), pp. 1783–1793.

[28] Benjamin Kerr, Margaret A Riley, Marcus W Feldman, and Brendan JM Bohannan. "Local dispersal promotes biodiversity in a real-life game of rock–paper–scissors". In: *Nature* 418.6894 (2002), p. 171.

[29] M Demerec and Uj Fano. "Bacteriophage-resistant mutants in Escherichia coli". In: *Genetics* 30.2 (1945), p. 119.

[30] Brendan JM Bohannan and Richard E Lenski. "Linking genetic change to community evolution: insights from studies of bacteria and bacteriophage". In: *Ecology letters* 3.4 (2000), pp. 362–377.

[31] Britt Koskella, Derek M Lin, Angus Buckling, and John N Thompson. "The costs of evolving resistance in heterogeneous parasite environments". In: *Proceedings of the Royal Society of London B: Biological Sciences* (2011), rspb20112259.

[32] E Chapman-McQuiston and XL Wu. "Stochastic receptor expression allows sensitive bacteria to evade phage attack. Part I: experiments". In: *Biophysical journal* 94.11 (2008), pp. 4525–4536.

[33] E Chapman-McQuiston and XL Wu. "Stochastic receptor expression allows sensitive bacteria to evade phage attack. Part II: theoretical analyses". In: *Biophysical journal* 94.11 (2008), pp. 4537–4548.

[34] Nina Molin Høyland-Kroghsbo, Rasmus Baadsgaard Mærkedahl, and Sine Lo Svenningsen. "A quorum-sensing-induced bacteriophage defense mechanism". In: *MBio* 4.1 (2013), e00362–12.

[35] John Yin. "A quantifiable phenotype of viral propagation". In: *Biochem. Biophys. Res. Comm.* 174.2 (1991), pp. 1009–1014.

[36] Lucia Vidakovic, Praveen K Singh, Raimo Hartmann, Carey D Nadell, and Knut Drescher. "Dynamic biofilm architecture confers individual and collective mechanisms of viral protection". In: *Nature microbiology* 3.1 (2018), p. 26.

[37] Matthew Simmons, Knut Drescher, Carey D Nadell, and Vanni Bucci. "Phage mobility is a core determinant of phagebacteria coexistence in biofilms". In: *The ISME Journal* 12.2 (2018), pp. 531–543. DOI: 10.1038/ismej.2017.190.

[38] AH Doermann. "Lysis and lysis inhibition with Escherichia coli bacteriophage". In: *J. Bacteriol.* 55.2 (1948), p. 257.